

## Numerical Simulation of Nonlinear Dynamical Behaviors of Active Magnetic Bearing-rotor System

Miao Lu<sup>1</sup>, Lingmei Zhang<sup>2</sup>, Baocang Sun<sup>3,\*</sup>, Huijuan Fan<sup>4</sup>  
<sup>1,2,3,4</sup>Faculty of Science, Jiangsu University, Zhenjiang, Jiangsu, 212013, P.R. China

<sup>\*</sup>Aeolus Tyre Co, LTD. Jiaozuo, 454003, P.R. China

*(Received 1 January 2006, accepted 15 June 2006)*

**Abstract:** In this paper, the nonlinear dynamical behaviors of an active magnetic bearing-rotor system are investigated using numerical simulation. Firstly, the nonlinear magnetic force is obtained by Taylor series. Secondly, the primary-internal resonance of an AMBRS (active magnetic bearing) -rotor system is studied with the help of Lung-Kutta method. To analyze the motion characters of system, some Poincare maps are drawn and several Lyapunov exponents are calculated. The conclusion: the chaotic phenomenon by period-doubling bifurcation and ring surface break period-doubling bifurcation are respectively discovered. Especially, a chaotic attractor on Poincare map that is extremely sensitive to initial value is discovered.

**Keywords:** active magnetic bearing-rotor system; nonlinear dynamics; bifurcation; chaos

### 1 Preface

Active magnetic bearing-rotor system (AMBRS) is a result that has been synthesized by mechanics, machinery, electronics and control science. The superiorities of AMBRS are having no power consumption caused by friction and material fatigue by wearing ([1]). It has been used in many rotational machines ([1, 2]).

A number of research results of the dynamic behavior and its control of AMBRS have been already obtained, but the results were mainly based on linear theory ([3]). If the rotator inclines or control quantum changes heavily, behavior of nonlinearity will be very important ([3, 4, 5, 9]). In this paper, complicated phenomenon of nonlinear dynamic behavior in an eight-pole AMBRS is introduced. Our investigations consist in choosing electric current as control quantum; obtaining the third power of nonlinear magnetic force by Taylor series; considering the effect of the rotator; the primary-internal resonance of an AMBRS are studied with the help of Lung-Kutta method.

### 2 Magnetic force

The Fig 1 is a schematic drawing of AMBRS. The stator has eight poles. They have the same structure and full circle numbers of coil. According to electromagnetism theory ([2]), the force of each pole is given as (2.1).

$$F_i = \frac{1}{4} \mu_0 N^2 A_\alpha \left( \frac{I_i}{C_i} \right)^2 \cos \beta \quad i = 1, 2, \dots, 8 \quad (2.1)$$

<sup>1</sup>Corresponding author. E-mail address: mlu@ujs.edu.cn

Here  $\mu_0$  is the magnetic inductivity in the vacuum,  $N$  the full circle number of coil's,  $A_\alpha$  the cross setioc area of magnetic pole,  $C_i$  the gap between pole and rotator;  $I_i$  current throw coil; ( $\alpha, \beta$  seen in fig.1.)

$$\begin{aligned} C_{1,5} &= C_0 \pm x \sin \alpha \mp y \cos \alpha & C_{4,8} &= C_0 \pm x \sin \alpha \pm y \cos \alpha \\ C_{2,6} &= C_0 \pm x \cos \alpha \mp y \sin \alpha & C_{3,7} &= C_0 \pm x \cos \alpha \pm y \sin \alpha \end{aligned}$$

$C_0$  the mean gap between pole and rotator.

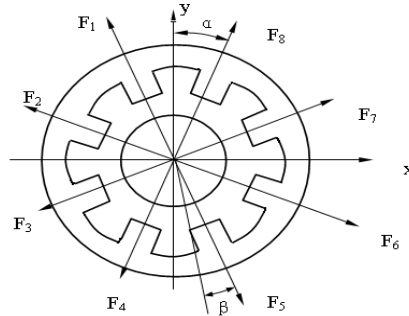


Figure 1: Simple map of active magnetic bearing structure

Current throw coil  $I_i$  equal to the sum of inclined current  $I_0$  and the controlled one  $i$ . For the AMBRS arranged in fig.1. the current passing through each coil can be given as

$$\begin{aligned} I_1 &= I_8 = I_0 - i_y, & I_4 &= I_5 = I_0 + i_y \\ I_6 &= I_7 = I_0 - i_x, & I_3 &= I_2 = I_0 + i_x \end{aligned} \quad (2.2)$$

Choose the controlled current PD as Varity thus

$$i_x = k_p x + k_d \dot{x} \quad i_y = k_p y + k_d \dot{y} \quad (2.3)$$

$k_p$  is the propotional coefficiene and the  $k_d$  the differential one.

Substituting (2.2) an (2.3) into (2.1), the force of each pole is obtained, and the resultant force acting on the rotator is gotten by vector-sum.

$$\begin{aligned} F_x &= (F_6 + F_7 - F_2 - F_3) \cos \alpha + (F_5 + F_8 - F_1 - F_4) \sin \alpha \\ F_y &= (F_1 + F_8 - F_4 - F_5) \cos \alpha + (F_2 + F_7 - F_3 - F_6) \sin \alpha \end{aligned} \quad (2.4)$$

### 3 Mathematic model

The differential equation of the AMBRS shown as fig.1 is (To simplify our discussion put the AMBRS relected).

$$\begin{aligned} m \ddot{x} + c \dot{x} &= F_x + m e \Omega^2 \cos \Omega t \\ m \ddot{y} + c \dot{y} &= F_y + m e \Omega^2 \sin \Omega t \end{aligned} \quad (3.1)$$

Here,  $m$  is the half of rotator mass,  $c$  the damping,  $e$  the length of the rotator's incline,  $\Omega$  the angular speed of the rotator incline,  $F_x$  is portion to  $x$  direction of the force acting on rotator, and  $F_y$  to  $y$  direction,  $(\cdot)$  denotes differential coefficient with respect to time  $t$ .

In order to analyze the portion effect of the behavior of AMBRS, we extend  $F_x$  and  $F_y$  as Taylor series at point (0,0), and simplify the series by remaining the low power term. Put (2.1) into non-measure form  $X = x/C_0, Y = y/C_0, i_x = I_0 I_x, i_y = I_0 I_y, t = B\tau, \Omega = \omega/B$ , and  $(\cdot)$  denotes the derivative with respect to  $\tau$  after some illation, (3.1) becomes

$$\begin{aligned}
 X'' + 2\mu X' + \omega_0^2 X - (\alpha_1 X^3 + \alpha_2 XY^2 + \alpha_3 X^2 X' + \alpha_4 X' Y^2 \\
 + \alpha_5 XY'^2 + \alpha_6 X X'^2 + \alpha_7 X Y Y') = \rho \cos \omega \tau \\
 Y'' + 2\mu Y' + \omega_0^2 Y - (\alpha_1 Y^3 + \alpha_2 X^2 Y + \alpha_3 Y^2 Y' + \alpha_4 X^2 Y' \\
 + \alpha_5 X'^2 Y + \alpha_6 Y Y'^2 + \alpha_7 X X' Y) = \rho \sin \omega \tau
 \end{aligned}
 \tag{3.2}$$

$$\begin{aligned}
 2\mu &= 8d \cos^3 \alpha + c_1 & \omega_0^2 &= 8(p \cos \alpha - 1) \\
 \alpha_1 &= 16(\cos^4 \alpha + \sin^4 \alpha) - 24p \cos^3 \alpha + 8p^2 \cos^2 \alpha \\
 \alpha_2 &= 96 \cos^2 \alpha \sin^2 \alpha - 72p \cos \alpha \sin^2 \alpha + 8p^2 \sin^2 \alpha \\
 \alpha_3 &= -24d \cos^3 \alpha + 16pd \cos^2 \alpha & \alpha_4 &= -24d \cos \alpha \sin^2 \alpha & \alpha_5 &= 8d^2 \sin^2 \alpha \\
 \alpha_6 &= 8d^2 \cos^2 \alpha, & \alpha_7 &= 16pd \sin^2 \alpha - 48d \sin^2 \alpha \cos \alpha \\
 p &= \frac{k_p C_0}{I_0}, & d &= \frac{k_d C_0}{I_0 B}, & B^2 &= \frac{4m C_0^3}{\mu_0 N^2 A_\alpha I_0^2}, & c_1 &= \frac{c C_0}{B}, & \rho &= \frac{e w^2}{C_0}
 \end{aligned}
 \tag{3.3}$$

Obviously, (3.2) is a two-degree system containing third power of variation and is under the situation of 1 : 1 inner resonance.

### 4 Numerical simulation

Using the method of Lung-Kutta, we simulated (3.2), and non-menagere incline  $\rho$  is chosen as bifurcation. To simplify the calculation, we take  $\omega = \omega_0 = 1$  and substitute  $\alpha = \pi/8$  (the eight poles arranged evenly) into(7), and get  $p = 1.217$ . And let  $d = 0.005, c_1 = 0.001$ . We can get rest coefficient by taking them into eq.7. The (3.2) was integrated by taking time-step  $0.01\pi$ , and using four power Lunge-Kutta.

The result shows that, when the system being in the situation of the one-third time second resonance and three time sup- resonance, it has very simple appearance, mainly indicating synchronous period motion. When the system is being in the primary-internal resonance, the behavior is very abundant.

From bifurcation maps Fig.2(a) and its partial-detail Fig2.(b) and Fig2.(c), we can know the motion regulation of the system which varies with the increase of the non-menageries incline  $\rho$ : synchronous periodic motion  $\rightarrow$  form Hopf bifurcation to quasi-period motion  $\rightarrow$  ring surface period-doubling bifurcation on Poincare sections  $\rightarrow$  from ring surface break to chaos  $\rightarrow 3T$  periodic motion on Poincare sections(including KT periodic window)  $\rightarrow 7T$  periodic motion  $\rightarrow$  from incessant period-doubling bifurcation to chaos  $\rightarrow$  be off chaos from return period-doubling bifurcation  $\rightarrow$  from period-doubling bifurcation to chaos motion  $\rightarrow 13T$  periodic motion  $\rightarrow$  from incessant period-doubling bifurcation to chaos  $\rightarrow 6T$  periodic motion  $\rightarrow$  from period-doubling bifurcation to chaos.

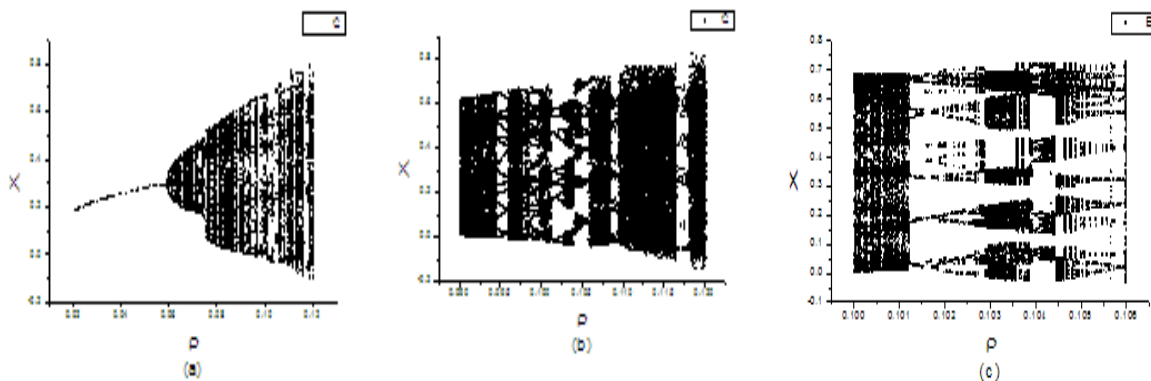


Figure 2: Bifurcation maps

To analyze the behavior of the system exactly, several different Poincare maps are made. Fig3(a)-Fig3(d) show that, when the non-menagere incline increase, the ring on Poincare sections varies from one to two, four,

even break, so, obviously it is from ring surface break (ring surface period-doubling bifurcation) to chaos. Fig3(e) indicates the system is quasi-period motion ( $3T$  periodic motion on Poincare sections) at this time. Fig3(d)-Fig3(f) are Poincare maps when  $\rho = 0.07445$  and  $0.114$ , which is typical chaotic attractor. The largest Lyapunov exponents are  $0.0451$  and  $0.198$  respectively, it is chaotic motion. Our investigation

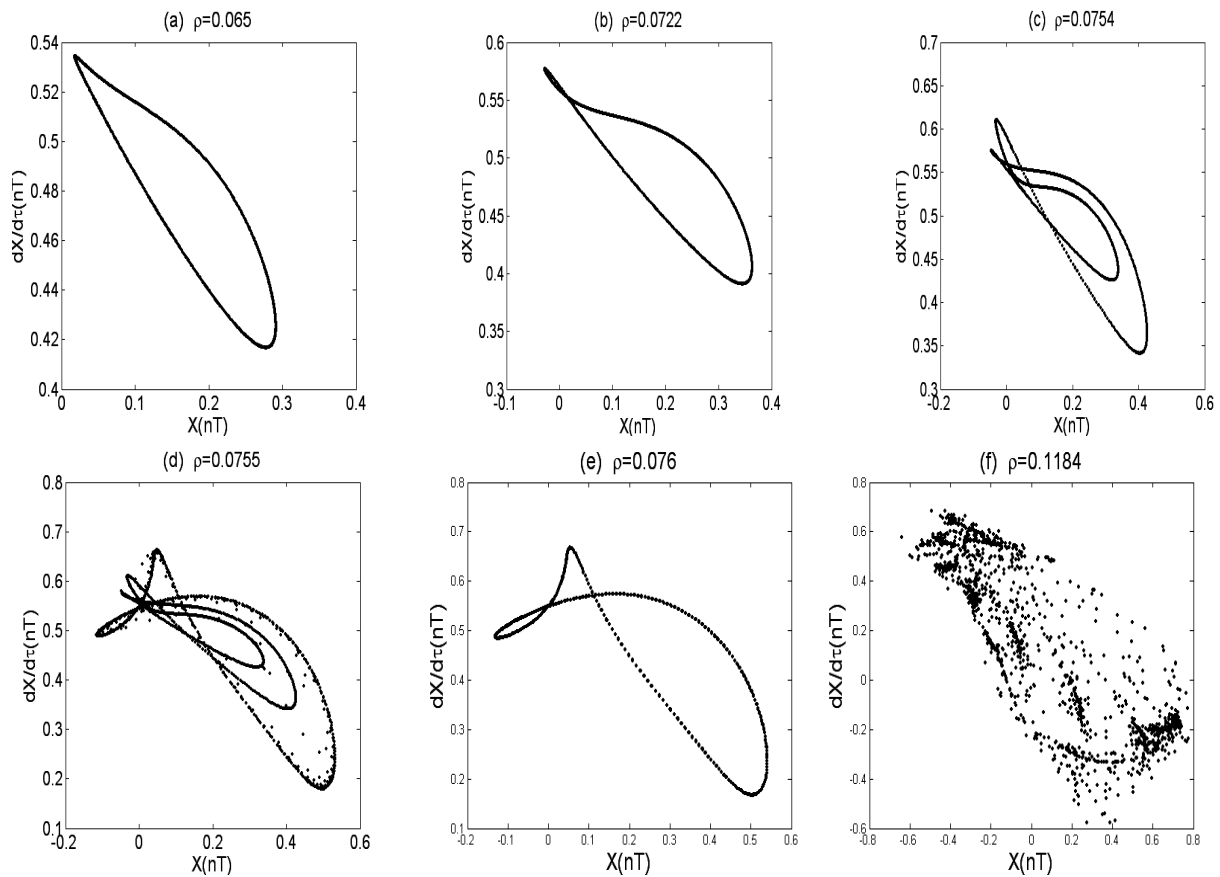


Figure 3: Poincaré maps of several points

indicates that, when  $\rho = 0.118$ , chaotic attractor of Poincaré section is very sensitive to initial value of  $\rho$ . In the region which radius is  $0.8$  on the  $(x, y)$  plane, we choose more than one hundred initial conditions, and obtain more than ten types of chaotic attractors (six different Poincaré maps are given in fig.4).

## 5 Conclusions

(1) The nonlinear dynamical behaviors of an active magnetic bearing-rotor system are investigated using numerical simulation when the system being in the primary-internal resonance, and the chaotic phenomenon by ring surface break and period-doubling bifurcation is discovered with increase of the non-menageriee incline. Mostly the chaotic attractor of Poincaré section is stable, but the chaotic attractor is very sensitive to initial value of  $\rho$  when it is with range of specific parameter.

(2) The results discovered in this paper are useful to explain the nonlinear dynamical phenomenon and to diagnosis problems of an active magnetic bearing-rotor system.

(3) The bifurcation (chosen as non-menageriee incline  $\rho$ ) is effected by many factors. Though the nonlinear dynamical behaviors of a active magnetic bearing-rotor system is very complicated, we can prevent its appearance by choosing suitable parameter.

## Acknowledgements

This research is supported by the National Defense Fundamental Science Foundation of China (No.A2520060236).

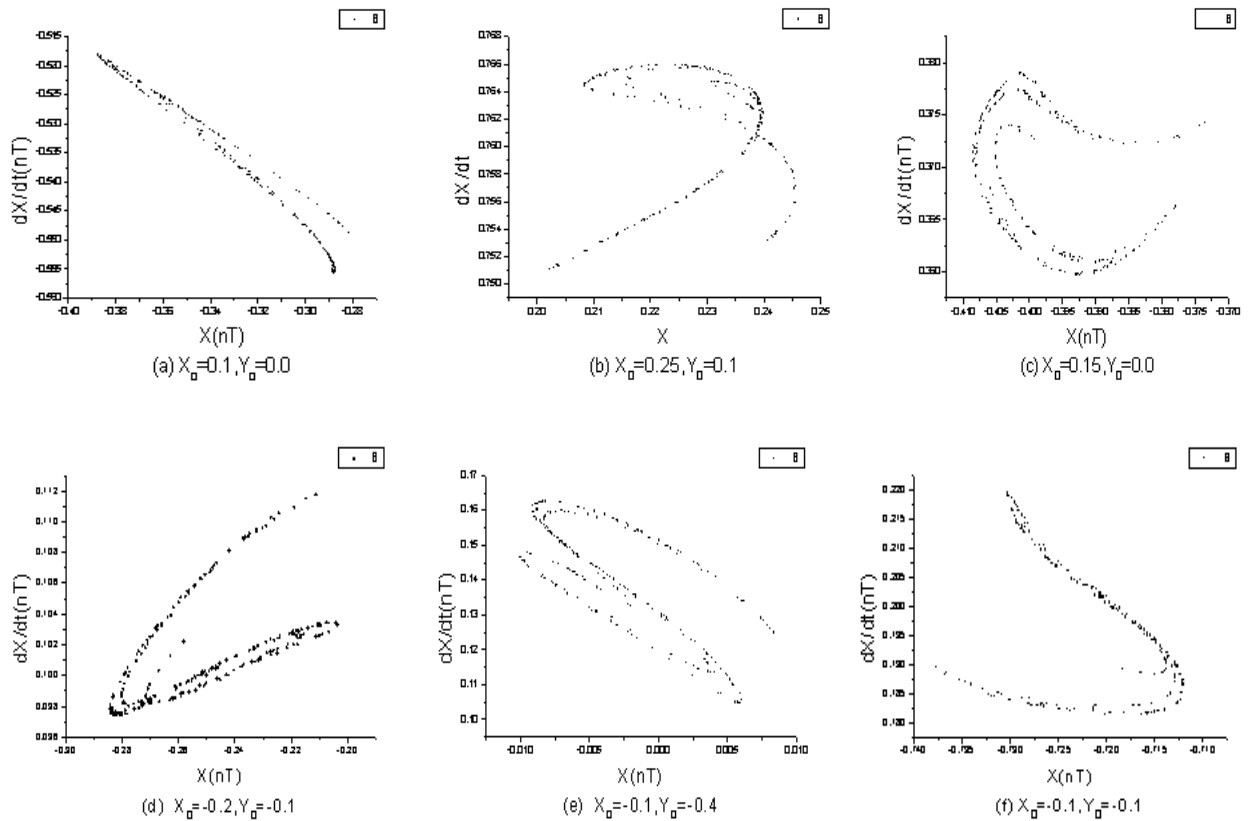


Figure 4: Several different Poincaré Maps

## References

- [1] Wen Bangchun, Gu Jialiu, Xia Songbo, et al: Higher rotor dynamics theory. *Technology and Application*. Mechanical Industry Publishing House: Beijing (2000)
- [2] Yu Lie, Liu Heng: Bearing-rotor system dynamics. Xi'an Jiaotong University Publishing House: Xi'an (2001)
- [3] M Chinta, A B Palazzolo: Stability and bifurcation of motion on a magnetic bearing. *Journal of Sound and Vibration*. 214(5), 93-803 (1998)
- [4] J C Ji, L YU, A Y Leung: Bifurcation behavior of a rotor in active magnetic bearings. *Journal of Sound and Vibration*. 235(2), 133-151 (2000)
- [5] J C Ji, Hansen: Non-linear oscillations of a Rotor in active magnetic bearings. *Journal of Sound and Vibration*. 240(4), 599-612 (2001)
- [6] Qinsheng Bi: Dynamics and modulated : Chaos for two coupled oscillators. *Int Journal of Bifurcation and Chaos*. 14(1), 337-346 (2004)
- [7] Xu Longxiang, Zhou Bo: The current situation and development trend for more-electric gas turbine engines. *Journal of Aerospace Power*. 18(1), 51-59 (2002)
- [8] Yang Shaopu, Shen Yongjun: Bifurcation and singularity of dynamical system with hysteretic nonlinearity. *Science Publishing House: Beijing* (2003)
- [9] Mei Sun, Lixin Tian, Jun Xu: Time-delayed feedback control of the energy resource chaotic system. *International Journal of Nonlinear Science*. 1(3), 172-177 (2006)